Gigahertz frequency comb from a diode-pumped solid-state laser

Alexander Klenner,[1,*] Stéphane Schilt,[2] Thomas Südmeyer,[2] and Ursula Keller[1]

[1]*Department of Physics, Institute for Quantum Electronics, ETH Zurich, 8093 Zurich, Switzerland*
[2]*Laboratoire Temps-Fréquence, Université de Neuchâtel, 2000 Neuchâtel, Switzerland*
[*]*klenner@phys.ethz.ch*

Abstract: We present the first stabilization of the frequency comb offset from a diode-pumped gigahertz solid-state laser oscillator. No additional external amplification and/or compression of the output pulses is required. The laser is reliably modelocked using a SESAM and is based on a diode-pumped Yb:CALGO gain crystal. It generates 1.7-W average output power and pulse durations as short as 64 fs at a pulse repetition rate of 1 GHz. We generate an octave-spanning supercontinuum in a highly nonlinear fiber and use the standard f-to-$2f$ carrier-envelope offset (CEO) frequency f_{CEO} detection method. As a pump source, we use a reliable and cost-efficient commercial diode laser. Its multi-spatial-mode beam profile leads to a relatively broad frequency comb offset beat signal, which nevertheless can be phase-locked by feedback to its current. Using improved electronics, we reached a feedback-loop-bandwidth of up to 300 kHz. A combination of digital and analog electronics is used to achieve a tight phase-lock of f_{CEO} to an external microwave reference with a low in-loop residual integrated phase-noise of 744 mrad in an integration bandwidth of [1 Hz, 5 MHz]. An analysis of the laser noise and response functions is presented which gives detailed insights into the CEO stabilization of this frequency comb.

©2014 Optical Society of America

OCIS codes: (320.6629) Supercontinuum generation; (140.3615) Lasers, ytterbium; (140.3480) Lasers, diode-pumped; (120.3940) Metrology; (140.3425) Laser stabilization; (140.4050) Mode-locked lasers.

References and links

1. H. R. Telle, G. Steinmeyer, A. E. Dunlop, J. Stenger, D. H. Sutter, and U. Keller, "Carrier-envelope offset phase control: A novel concept for absolute optical frequency measurement and ultrashort pulse generation," Appl. Phys. B **69**(4), 327–332 (1999).
2. U. Keller, "Ultrafast solid-state laser oscillators: a success story for the last 20 years with no end in sight," Appl. Phys. B **100**(1), 15–28 (2010).
3. D. J. Jones, S. A. Diddams, J. K. Ranka, A. Stentz, R. S. Windeler, J. L. Hall, and S. T. Cundiff, "Carrier-envelope phase control of femtosecond mode-locked lasers and direct optical frequency synthesis," Science **288**(5466), 635–639 (2000).
4. A. Apolonski, A. Poppe, G. Tempea, C. Spielmann, T. Udem, R. Holzwarth, T. W. Hänsch, and F. Krausz, "Controlling the Phase Evolution of Few-Cycle Light Pulses," Phys. Rev. Lett. **85**(4), 740–743 (2000).
5. L.-S. Ma, Z. Bi, A. Bartels, L. Robertsson, M. Zucco, R. S. Windeler, G. Wilpers, C. Oates, L. Hollberg, and S. A. Diddams, "Optical Frequency Synthesis and Comparison with Uncertainty at the $10^{(-19)}$) Level," Science **303**(5665), 1843–1845 (2004).
6. C. J. Campbell, A. G. Radnaev, A. Kuzmich, V. A. Dzuba, V. V. Flambaum, and A. Derevianko, "Single-Ion Nuclear Clock for Metrology at the 19th Decimal Place," Phys. Rev. Lett. **108**(12), 120802 (2012).
7. B. A. Wilt, L. D. Burns, E. T. Wei Ho, K. K. Ghosh, E. A. Mukamel, and M. J. Schnitzer, "Advances in Light Microscopy for Neuroscience," Annu. Rev. Neurosci. **32**(1), 435–506 (2009).
8. T. Ideguchi, S. Holzner, B. Bernhardt, G. Guelachvili, N. Picqué, and T. W. Hänsch, "Coherent Raman spectro-imaging with laser frequency combs," Nature **502**(7471), 355–358 (2013).
9. M. T. Murphy, T. Udem, R. Holzwarth, A. Sizmann, L. Pasquini, C. Araujo-Hauk, H. Dekker, S. D'Odorico, M. Fischer, T. W. Hänsch, and A. Manescau, "High-precision wavelength calibration of astronomical spectrographs with laser frequency combs," Mon. Not. R. Astron. Soc. **380**(2), 839–847 (2007).
10. N. R. Newbury, "Searching for applications with a fine-tooth comb," Nat. Photonics **5**(4), 186–188 (2011).

11. T. Herr, V. Brasch, J. D. Jost, C. Y. Wang, N. M. Kondratiev, M. L. Gorodetsky, and T. J. Kippenberg, "Temporal solitons in optical microresonators," Nat. Photonics **8**(2), 145–152 (2013).
12. Y. Okawachi, M. R. E. Lamont, K. Luke, D. O. Carvalho, M. Yu, M. Lipson, and A. L. Gaeta, "Bandwidth shaping of microresonator-based frequency combs via dispersion engineering," Opt. Lett. **39**(12), 3535–3538 (2014).
13. A. Bartels, D. Heinecke, and S. A. Diddams, "10-GHz Self-Referenced Optical Frequency Comb," Science **326**(5953), 681 (2009).
14. D. E. Spence, P. N. Kean, and W. Sibbett, "60-fsec pulse generation from a self-mode-locked Ti:sapphire laser," Opt. Lett. **16**(1), 42–44 (1991).
15. G. Steinmeyer, D. H. Sutter, L. Gallmann, N. Matuschek, and U. Keller, "Frontiers in Ultrashort Pulse Generation: Pushing the Limits in Linear and Nonlinear Optics," Science **286**(5444), 1507–1512 (1999).
16. U. Keller, K. J. Weingarten, F. X. Kärtner, D. Kopf, B. Braun, I. D. Jung, R. Fluck, C. Hönninger, N. Matuschek, and J. Aus der Au, "Semiconductor saturable absorber mirrors (SESAMs) for femtosecond to nanosecond pulse generation in solid-state lasers," IEEE J. Sel. Top. Quantum Electron. **2**(3), 435–453 (1996).
17. A. Schlatter, B. Rudin, S. C. Zeller, R. Paschotta, G. J. Spühler, L. Krainer, N. Haverkamp, H. R. Telle, and U. Keller, "Nearly quantum-noise-limited timing jitter from miniature Er:Yb:glass lasers," Opt. Lett. **30**(12), 1536–1538 (2005).
18. S. Schilt, V. Dolgovskiy, N. Bucalovic, C. Schori, M. C. Stumpf, G. Domenico, S. Pekarek, A. E. H. Oehler, T. Südmeyer, U. Keller, and P. Thomann, "Noise properties of an optical frequency comb from a SESAM-mode-locked 1.5-μm solid-state laser stabilized to the 10−13 level," Appl. Phys. B **109**, 1–12 (2012).
19. I. Hartl, H. A. McKay, R. Thapa, B. K. Thomas, A. Ruehl, L. Dong, and M. E. Fermann, "Fully Stabilized GHz Yb-Fiber Laser Frequency Comb," in *Advanced Solid-State Photonics* (Denver, Colorado, USA, 2009), p. MF9.
20. H.-W. Chen, G. Chang, S. Xu, Z. Yang, and F. X. Kärtner, "3 GHz, fundamentally mode-locked, femtosecond Yb-fiber laser," Opt. Lett. **37**(17), 3522–3524 (2012).
21. C. A. Zaugg, A. Klenner, M. Mangold, A. S. Mayer, S. M. Link, F. Emaury, M. Golling, E. Gini, C. J. Saraceno, B. W. Tilma, and U. Keller, "Gigahertz self-referenceable frequency comb from a semiconductor disk laser," Opt. Express **22**(13), 16445–16455 (2014).
22. U. Keller, "Recent developments in compact ultrafast lasers," Nature **424**(6950), 831–838 (2003).
23. A. Klenner, M. Golling, and U. Keller, "High peak power gigahertz Yb:CALGO laser," Opt. Express **22**(10), 11884–11891 (2014).
24. S. Pekarek, T. Südmeyer, S. Lecomte, S. Kundermann, J. M. Dudley, and U. Keller, "Self-referenceable frequency comb from a gigahertz diode-pumped solid-state laser," Opt. Express **19**(17), 16491–16497 (2011).
25. A. Klenner, M. Golling, and U. Keller, "A gigahertz multimode-diode-pumped Yb:KGW enables a strong frequency comb offset beat signal," Opt. Express **21**(8), 10351–10357 (2013).
26. N. Bucalovic, V. Dolgovskiy, M. C. Stumpf, C. Schori, G. Di Domenico, U. Keller, S. Schilt, and T. Südmeyer, "Effect of the carrier-envelope-offset dynamics on the stabilization of a diode-pumped solid-state frequency comb," Opt. Lett. **37**(21), 4428–4430 (2012).
27. A. Vernaleken, B. Schmidt, M. Wolferstetter, T. W. Hänsch, R. Holzwarth, and P. Hommelhoff, "Carrier-envelope frequency stabilization of a Ti:sapphire oscillator using different pump lasers," Opt. Express **20**(16), 18387–18396 (2012).
28. T. D. Mulder, R. P. Scott, and B. H. Kolner, "Amplitude and envelope phase noise of a modelocked laser predicted from its noise transfer function and the pump noise power spectrum," Opt. Express **16**(18), 14186–14191 (2008).
29. A. K. Chin and R. K. Bertaska, "Catastrophic Optical Damage in High-Power, Broad-Area Laser Diodes," in *Materials and Reliability Handbook for Semiconductor Optical and Electron Devices*, O. Ueda, and S. J. Pearton, eds. (Springer, New York, 2013), pp. 123–147.
30. A. Klenner, F. Emaury, C. Schriber, A. Diebold, C. J. Saraceno, S. Schilt, U. Keller, and T. Südmeyer, "Phase-stabilization of the carrier-envelope-offset frequency of a SESAM modelocked thin disk laser," Opt. Express **21**(21), 24770–24780 (2013).
31. J. Petit, P. Goldner, and B. Viana, "Laser emission with low quantum defect in Yb: CaGdAlO$_4$," Opt. Lett. **30**(11), 1345–1347 (2005).
32. J. Boudeile, F. Druon, M. Hanna, P. Georges, Y. Zaouter, E. Cormier, J. Petit, P. Goldner, and B. Viana, "Continuous-wave and femtosecond laser operation of Yb:CaGdAlO4 under high-power diode pumping," Opt. Lett. **32**(14), 1962–1964 (2007).
33. Y. Zaouter, J. Didierjean, F. Balembois, G. Lucas Leclin, F. Druon, P. Georges, J. Petit, P. Goldner, and B. Viana, "47-fs diode-pumped Yb^{3+}:CaGdAlO$_4$ laser," Opt. Lett. **31**(1), 119–121 (2006).
34. D. J. H. C. Maas, B. Rudin, A.-R. Bellancourt, D. Iwaniuk, S. V. Marchese, T. Südmeyer, and U. Keller, "High precision optical characterization of semiconductor saturable absorber mirrors," Opt. Express **16**(10), 7571–7579 (2008).
35. J. M. Dudley, G. Genty, and S. Coen, "Supercontinuum generation in photonic crystal fiber," Rev. Mod. Phys. **78**(4), 1135–1184 (2006).
36. G. Di Domenico, S. Schilt, and P. Thomann, "Simple approach to the relation between laser frequency noise and laser line shape," Appl. Opt. **49**(25), 4801–4807 (2010).

37. V. Dolgovskiy, N. Bucalovic, P. Thomann, C. Schori, G. D. Domenico, and S. Schilt, "Cross-influence between the two servo-loops of a fully-stabilized Er:fiber optical frequency comb," J. Opt. Soc. Am. B **29**(10), 2944–2957 (2012).

1. Introduction

Stabilized optical frequency combs based on ultrafast lasers [1–4] have enabled numerous breakthroughs in multiple fields of science. In optical metrology, frequency combs provide clockworks for atomic clocks and support measurements with fractional frequency uncertainties down to the 10^{-19} level [5, 6]. Molecular precision spectroscopy and nonlinear bio-imaging strongly benefit from high-speed and high-resolution data acquisition enabled by frequency combs [7, 8]. Finally, the calibration of astronomical spectrographs is improved in terms of accuracy and stability, thanks to the absolute frequency grid provided by a frequency comb [9, 10]. For most of these applications it is beneficial to increase the comb tooth spacing into the range of 1 to 10 GHz with high power per mode. Gigahertz frequency combs with high average output power of several watts provide substantially higher power per comb-mode as compared to conventional megahertz frequency combs or to microresonator-based frequency combs [11, 12].

Here we present the first self-referenced optical frequency comb from a gigahertz diode-pumped solid-state laser (DPSSL) oscillator, which in addition is achieved without any external amplifier or compressor. The various laser technologies based on Ti:sapphire, fibers, semiconductors, and DPSSLs have different competitive advantages. To-date, green-pumped Ti:sapphire and fiber lasers remain the most commonly-used frequency comb sources. Ti:sapphire lasers have reached up to 10-GHz repetition rate [13] and very high peak powers, but still require expensive and cumbersome green pump lasers. Also, Kerr-lens modelocking [14] enables ultrashort pulse durations of a few tens of femtoseconds, but relies on operating the laser at the edge of its stability range [15]. In contrast semiconductor saturable absorber mirrors (SESAM) provides stable and reliable modelocking [16]. In addition, SESAM modelocked DPSSLs can offer quantum-noise limited performance [17] and lower noise in frequency comb generation compared to typical fiber lasers [18]. Furthermore, moving fiber-laser-based frequency combs into the gigahertz regime is very challenging [19, 20]. Novel ultrafast semiconductor lasers look very promising but at this point still require additional external amplifiers and compressors [21]. Therefore DPSSLs stand out as particularly well-suited for gigahertz frequency combs and represents a promising alternative to the established frequency comb technologies. They are able to deliver high optical power from low-noise oscillators and can be directly diode-pumped with high-power laser diodes, which reduces the system complexity and increases their robustness and reliability. In addition, they benefit from self-starting stable SESAM-modelocking [2, 16, 22].

Recent advances in SESAM-modelocked gigahertz DPSSLs make them comparable to Ti:sapphire lasers in terms of peak power and pulse energy. For example, pulse durations below 60 fs in combination with high peak powers of up to 24 kW at 1.8 GHz repetition rate have been demonstrated with a SESAM-modelocked Yb:CALGO laser [23]. This performance is sufficient for coherent supercontinuum (SC) generation in standard photonic crystal fibers (PCFs) as demonstrated by the successful detection of a CEO frequency beat signal from SESAM modelocked Yb:KGW lasers [1, 24, 25]. However, self-referencing of such a DPSSL has not been demonstrated so far, and we have learned that the detection of a CEO beat signal with a high signal-to-noise ratio (SNR, e.g. 25 dB) alone is not sufficient for comb stabilization [26]. In addition, there has been some general concern that highly multi-transverse-mode pump laser diodes have a higher intensity noise than single-mode laser diodes, which is partly transferred to the modelocked laser and converted into CEO phase noise [27, 28]. However, high-power multi-spatial-mode pump diodes offer multiple advantages. First, the robustness and reliability of industrial-grade laser diodes is superior to the more fragile single-mode tapered laser diodes [29]. Furthermore, the laser diodes'

compactness greatly reduces the overall size of the laser system and allows for very compact frequency combs. Finally, the available pump power is basically only limited by the number of emitters coupled to the multi-mode fiber and can reach up to several kilowatts, nowadays. Recently, we demonstrated the first CEO-stabilization of a thin disk oscillator, which generally requires a multi-spatial-mode pumping scheme. Despite that pumping scheme, the 65-MHz thin disk laser operated at low noise and offered a narrow free-running CEO beat linewidth, which enabled us to achieve a tight CEO phase-lock by applying feedback to the pump diode current with a bandwidth of only up to 40 kHz [30].
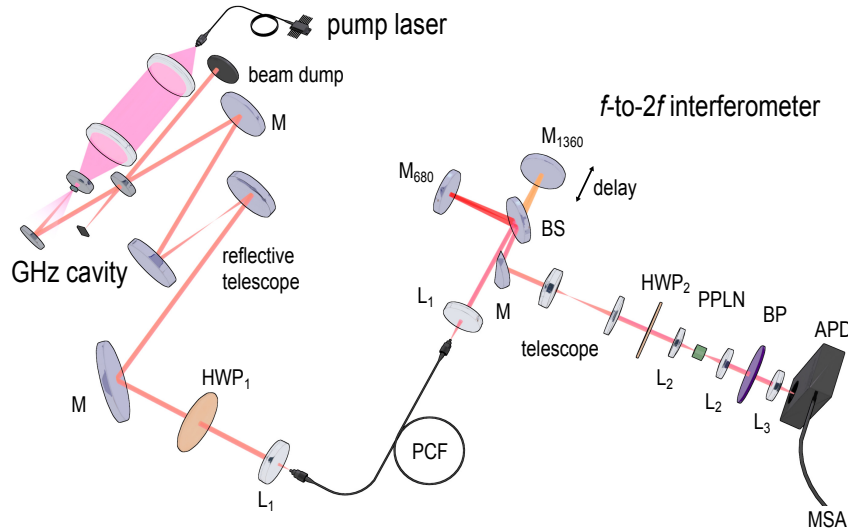

Fig. 1. Full experimental setup showing the diode-pumped 1-GHz SESAM-modelocked Yb:CALGO oscillator, the PCF and the *f*-to-2*f* interferometer. M: silver mirror; M680, M1360: Notch-type mirror for 680 nm, 1360 nm wavelengths; BS: dichroic beam splitter; HWP1, HWP2: half-wave-plate for 1050 nm and 1310 nm; L1, L2, L3: lenses (focal lengths: 3.1 mm, 40 mm and 50 mm); PCF: photonic crystal fiber (see text for specs.); PPLN: periodically poled lithium niobate for second harmonic generation of 1360 nm; BP: bandpass filter for 680 nm, APD: avalanche photodiode with 1-GHz bandwidth; MSA: microwave spectrum analyzer.

The Yb:CALGO laser used for the gigahertz frequency comb presented here is pumped with a strongly multi-spatial-mode laser diode, which enables high-power performance with 1.7 W average output power and optimized SESAM-modelocking enabled a pulse duration of ≈60 fs. As a result, the generation and detection of the CEO beat of the gigahertz comb is achieved without using any additional pulse compression or amplification. But the fluctuations of the free-running CEO frequency result in a beat-note that is about 100-times broader as compared to the case of the thin disk laser in [30]. This significantly increases the demands on the electronic bandwidth for the phase locked loop (PLL). Nevertheless, a tight CEO phase-lock was obtained using a simple feedback to the current of the multi-mode pump laser. This proves that frequency comb self-referencing is not prevented by multi-mode pumping, but relies on a proper laser cavity design and appropriate electronic feedback. Our noise analysis and characterization of the laser transfer functions reveal the important requirements for the CEO-stabilization of such compact frequency combs.

2. 1-GHz DPSSL performance and optical setup

The DPSSL used in our experiment is similar to the one published in [23]. The length of the compact Z-shaped cavity was slightly increased to about 150 mm resulting in a pulse repetition rate of 1.0 GHz. The complete optical setup, including the laser oscillator,

supercontinuum generation and CEO beat detection, is shown in Fig. 1. A commercial fiber-coupled multi-transverse-mode laser diode is used as a pump source (LIMO60-F200-DL980-LM, Lissotschenko Mikrooptik GmbH). A single diode-array with ten emitters is coupled to the multi-mode fiber with an overall efficiency of 80%. The fiber core diameter is ≈100 μm and its numerical aperture is ≈0.22, resulting in low-brightness output with an M^2 of about 32. No expensive wavelength-stabilizing element, e.g., a volume holographic grating, is included to stabilize the pump spectrum. The maximum pump power is 60 W, of which only a fraction of about 8 W is used in our experiment. The 4-nm broad pump spectrum is centered at around 980 nm, ideally suited to pump Yb-doped CALGO [31–33].
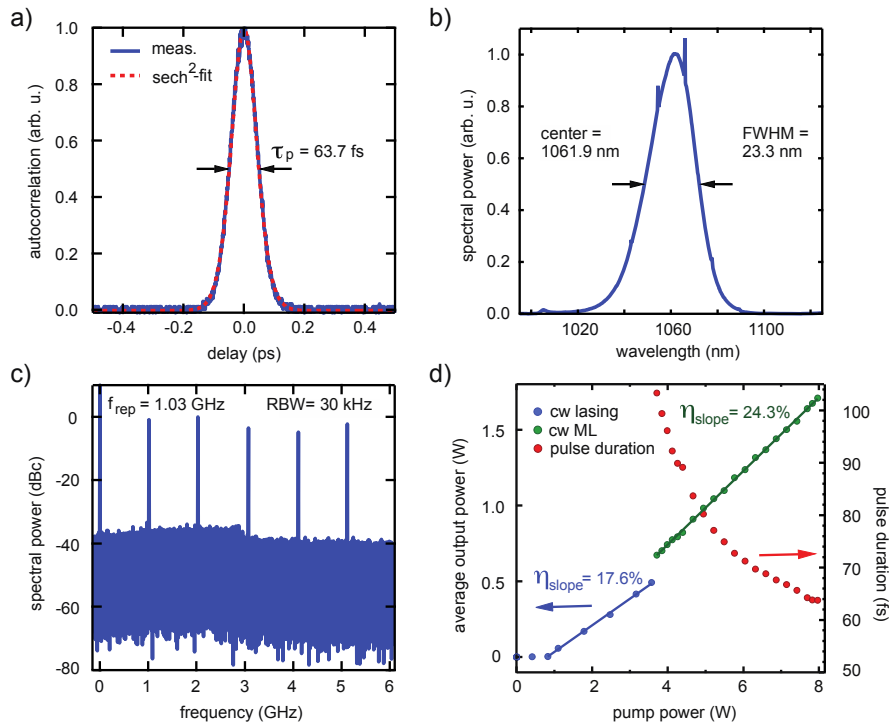

Fig. 2. SESAM-modelocked multi-spatial-mode pumped Yb:CALGO laser at 1-GHz pulse repetition rate: (a) Intensity autocorrelation showing 63.7-fs pulses obtained at an average output power of 1.7 W; (b) The corresponding optical spectrum spans 23.3 nm centered at around 1061.9 nm; (c) Microwave spectrum showing the fundamental and harmonics of the pulse repetition rate in a 6-GHz span (RBW = 30 kHz); (d) Total output power (left) and measured pulse duration (right) versus multimode pump power. At 3.6-W pump power, continuous-wave (cw) modelocking (ML) is reliably achieved.

The 2-mm long Yb:CALGO crystal is pumped through a dichroic flat end-mirror. A curved GTI-type mirror provides 400 fs^2 of negative group delay dispersion and transmits residual pump light, which reduces the thermal load of the cavity. A flat output-coupler was used as a folding mirror generating two output beams. In comparison to the previous configuration we presented in [23], the total output coupling rate was lowered to 2% to increase the cavity Q-factor and reduce the sensitivity to pump power fluctuations. One of the output beams is used for frequency comb stabilization, while the other beam can be used for frequency comb applications. Self-starting soliton modelocking is initiated and maintained using a SESAM, which was soldered on a passively cooled cupper heat sink. The SESAM is a single AlAs-embedded InGaAs quantum well with a saturation fluence of ≈11 μJ/cm^2 and a modulation depth of ≈1.4%. The precise SESAM characterization was

performed at room temperature with 95-fs pulses at 1051 nm with a setup described in detail by D. J. H. C. Maas et al. in [34].

In this configuration, the gigahertz laser generated pulses as short as 63.7 fs with a maximum average output power of 1.7 W equally distributed in the two laser outputs. The optical spectrum is centered at 1061.9 nm and spans over 23.3 nm (Figs. 2(a)–(d)). It shows additional cw components, which are emitted in the orthogonal polarization due to an imperfect polarization extinction by the biaxial gain crystal. The power of these cw components is <0.6% of the total average output power of the gigahertz frequency comb.

3. CEO frequency detection and transfer functions

For the CEO beat measurements we used the output of the gigahertz laser pulses with about 65-fs duration and an average output power of 500 mW and launched them into a 1-m long standard photonic crystal fiber (PCF, NL-3.2-945, NKT Photonics) with a coupling efficiency of about 80%. The PCF provides a nonlinear coefficient of 23 $(W\ km)^{-1}$ and anomalous dispersion for wavelengths above the zero dispersion wavelength (ZDW) at 945 nm. The dispersion curve used in the numerical simulations is given in Fig. 3(b). The supercontinuum is generated using an efficient spectral broadening process, called soliton fission [35]. Each laser pulse corresponds to a Nth-order soliton that is coupled into the PCF in the anomalous dispersion regime. The higher-order soliton propagates through the PCF and subsequently splits into N fundamental solitons, which propagate with their own group velocity and exhibit soliton self-frequency shifts to longer wavelength. In the normal dispersion regime, at wavelengths below the ZDW, dispersive waves are generated, which result from a resonant energy transfer from the solitons. The pulse and fiber parameters in our experiment result in an octave-spanning supercontinuum spectrum from 680 nm to 1360 nm.

Using a split-step Fourier-transform algorithm kindly provided by John M. Dudley [35], the SC generation was simulated, yielding an optical spectrum well matching the measured one. Using this numerical model, the first order temporal coherence (g^1) was calculated (Fig. 3(a) black, right axis). Due to the very short pulses, the octave-spanning spectrum is almost fully coherent. A useful metric to estimate the degree of coherence after the soliton fission process is the soliton order N that needs to be below 10, as introduced by Dudley et al. in 2006 [35]. For the parameters of our gigahertz laser and PCF, the soliton order is calculated to be 3.6, which is far below 10, indicating a high degree of coherence of the generated spectrum.

The coherent SC spectrum was sent into a quasi-common path *f*-to-2*f* interferometer for CEO beat generation and detection [1]. After frequency doubling of the long-wavelength part of the spectrum at 1360 nm, both 680-nm red laser beams were spectrally filtered and superimposed on a gigahertz bandwidth avalanche photodiode to generate the CEO beats. The measured microwave spectrum shows strong CEO beats at around 200 MHz and 800 MHz with more than 25-dB SNR in a 1-MHz resolution bandwidth (RBW) as depicted in Fig. 3(c). The free-running CEO beat has a full-width at half maximum (FWHM) of 2.1 MHz as shown in the inset of Fig. 3(c) in a 10-MHz span (100 averages, 30-kHz RBW). By modulating the pump power of the GHz-laser the CEO beat signals could be shifted by over 250 MHz without the need to adapt any alignment of the setup.
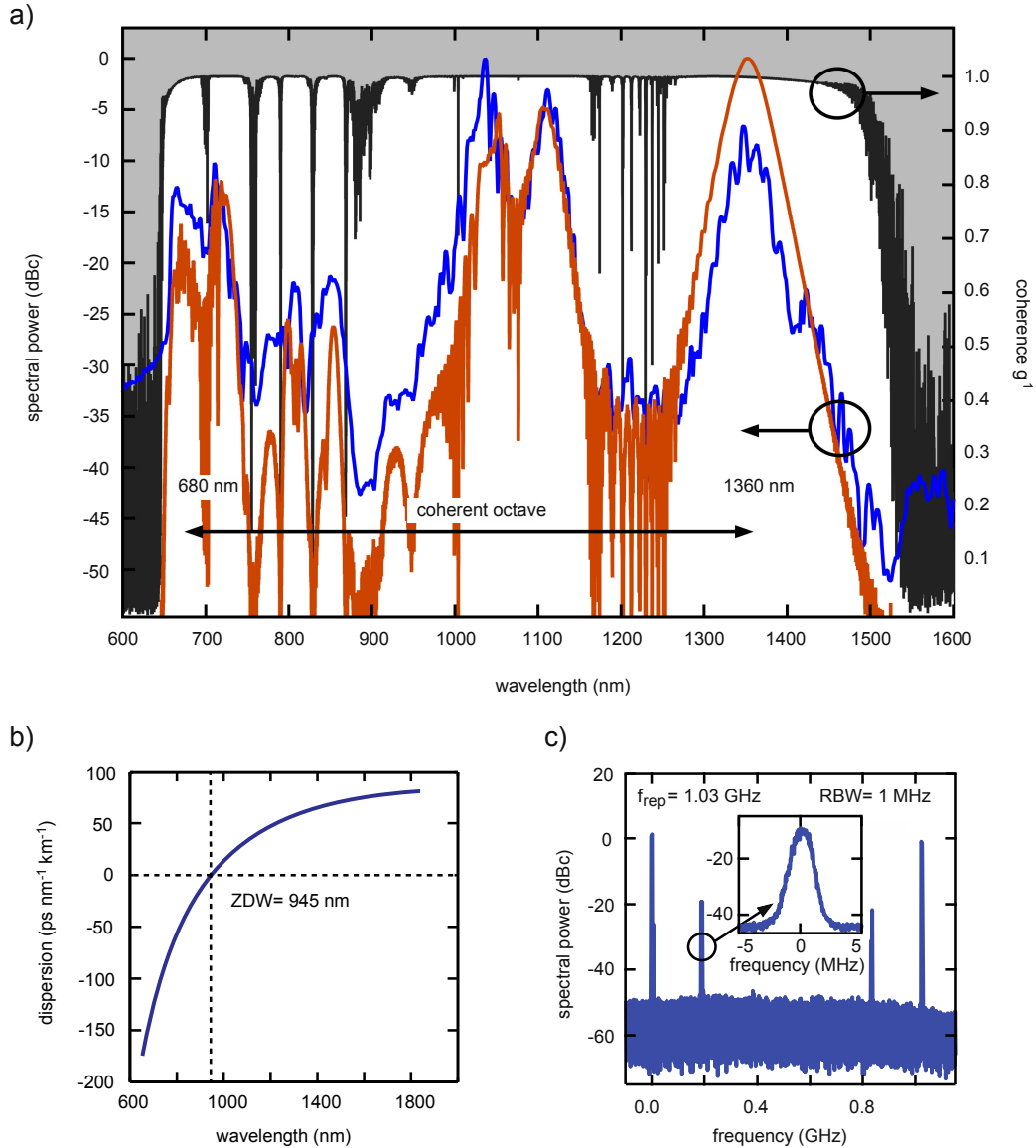
Fig. 3. Carrier-envelope offset (CEO) frequency generation and detection: (a) Measured (blue) and simulated (red) octave-spanning spectrum at the PCF output. The wavelength bands around 1360 nm and 680 nm are used for the f-to-$2f$ interferometry. The simulated first-order temporal coherence (g^1, right) is almost 100%, especially in the wavelength regions used for CEO beat detection. (b) PCF dispersion used for the supercontinuum generation simulations. Anomalous dispersion is provided above the zero dispersion wavelength at 945 nm. (c) Microwave spectrum of the free-running frequency comb showing the pulse repetition rate f_{rep} at 1 GHz as well as the CEO beat frequencies $f_{CEO,1}$ and $f_{CEO,2}$ at around 200 MHz and 800 MHz, respectively. The inset shows the free-running beat $f_{CEO,1}$ with a FWHM of 2.1 MHz in a 10-MHz span (RBW = 30 kHz, 100 averages).

CEO phase stabilization using a standard PLL based on a proportional-integrator-derivative (PID) servo-controller requires a linear system, i.e., a linear shift of f_{CEO} with the pump current. Optical feedback from the pump diode or GHz-laser back into the pump diode may increase its relative intensity noise (RIN) and cause a chaotic behavior. In order to

prevent reflections back into the pump laser, the anti-reflection-coated pump optics were slightly tilted from the pump beam and an additional dichroic mirror picked the leakage from the GHz-laser cavity. Furthermore, mechanical perturbations of the multimode fiber can lead to a strongly increased RIN. To mitigate this problem, a stainless steel fiber jacket was used, which greatly increased the robustness against environmental perturbations.

For our experiments, we always used a standard DC power supply (SM1850, DELTA Elektronika) rather than a highly expensive, low-noise current source. This DC supply can deliver sufficient energy to run the multi-mode pump diode, but it cannot be modulated rapidly (bandwidth << 1 kHz). As shown in Fig. 4(a), a fast current modulator was installed in parallel to the DC supply to be able to directly feedback to the current of the multimode pump for the frequency comb stabilization. An additional passive filter prevents AC currents to enter the DC supply. Additionally, the filter strongly reduces electrical noise from the DC power supply, such as the 50-Hz power line frequency and its harmonics, as well as frequencies of the switched-mode power supply. This approach reduces the complexity and costs in comparison to modulation via an additional external modulator (e.g., an acousto-optical modulator).

In Fig. 4(a), the electronic components used for the PLL are shown. The filtered and amplified microwave signal from the gigahertz avalanche photodiode at the output of the f-to-2f interferometer was compared to a microwave reference source in a digital phase detector. The output phase error signal was subsequently amplified by an analog PID servo-controller to generate the correction voltage that was converted into an electrical current applied to the multi-spatial-mode laser diode.

To verify that the above-described stabilization scheme provides the required modulation bandwidth to phase-lock the CEO frequency, we characterized the dynamic response of the laser system for a modulation of the pump current. In particular, we measured the amplitude and phase (Figs. 4 (b) and (c)) of the transfer functions of the CEO frequency (blue), GHz-laser power (green) and pump laser power (red). In this case the bandwidth is defined by the frequency where the phase-shift reaches −45 degrees, which corresponds to the 3-dB bandwidth of a first-order low-pass filter. Both the CEO frequency and the GHz-laser optical power have a bandwidth of ≈20-30 kHz, while the multi-mode pump power can be modulated with up to 500 kHz without significant amplitude change. This means that the limiting factor in the CEO frequency modulation does not arise from the pump diode driving electronics, but results from a first-order low-pass filter behavior originating from the effective upper-state lifetime and the photon lifetime in the GHz-cavity. Therefore, faster modulations are filtered by the GHz-cavity, thus limiting the achievable CEO feedback bandwidth. However, the same filtering effect is beneficial to damp high frequency noise components transferred from the pump diode to the modelocked laser, which contributes to limit the required feedback bandwidth.
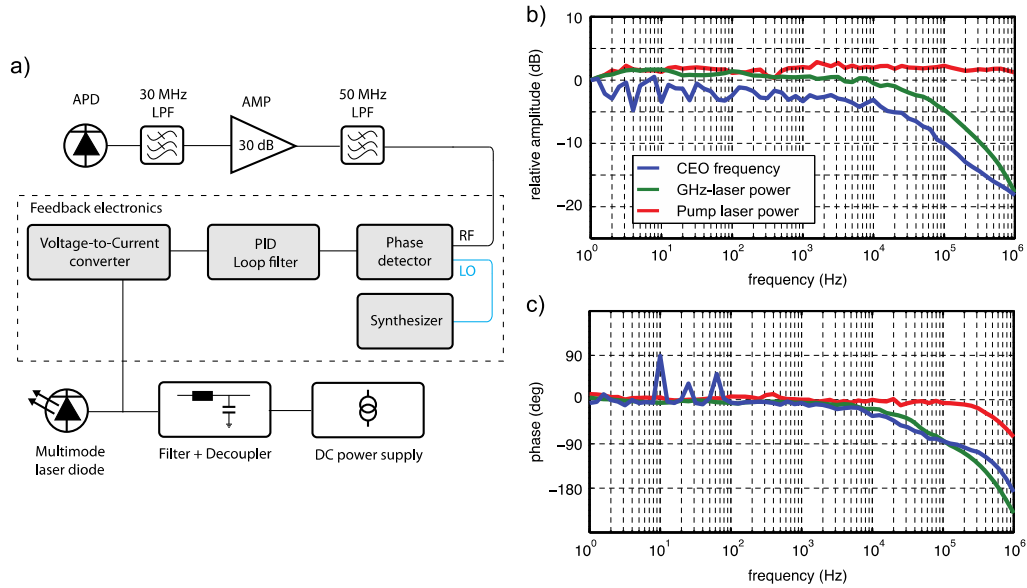
Fig. 4. (a) Schematic of the CEO-locking feedback loop electronics starting with the avalanche photodiode (APD) of the *f*-to-2*f* interferometer. The filtered and amplified CEO beat signal is sent to a digital phase detector. A microwave synthesizer is used as a reference to generate a phase error signal, which is amplified by a proportional-integrator-derivative (PID) servo-controller. The generated correction voltage is converted into a current modulation applied to the multi-spatial-mode pump diode laser. A DC power supply provides the required average pump current. A home-built filter reduces the electrical noise from the DC supply and avoids coupling of the AC current into the DC supply. (b) Normalized amplitude and (c) phase of the transfer functions of f_{CEO} (blue), of the GHz-laser output power (green) and of the optical pump power (red) as a function of the pump current modulation frequency.

4. CEO phase locking and noise characterization

The spectral analysis of the free-running CEO beat is shown in Fig. 5(a). The frequency noise power spectral density (PSD) of the CEO beat was measured using a frequency discriminator and a fast Fourier transform (FFT) spectrum analyzer. Damping of the electronic noise from the DC power supply led to a smooth CEO frequency noise spectrum without prominent excess noise peaks except at the 50-Hz power line originating from the analyzer itself. We used the concept of the β-separation line introduced by Di Domenico et al. [36] to estimate the minimum feedback loop bandwidth required to achieve a CEO phase-lock from its crossing point with the frequency noise PSD. In our experiment, this crossing point was estimated to be ≈150 kHz by extrapolation of the CEO frequency noise spectrum, as it lies beyond the 100-kHz upper limit of the FFT spectrum analyzer used in the measurement. This value exceeds the CEO frequency modulation bandwidth discussed in Section 3. Therefore, a phase-lead component needs to be introduced in the feedback loop in order to compensate for the phase-shift induced in the modulation of f_{CEO} via the pump current and to further extend the overall feedback loop bandwidth to be able to achieve a tight CEO lock. The derivative part of our analog PID loop filter is used for this purpose. We note that many commercially-available laser servo-controllers are pure PI filters, but without a derivative filter, so that a tight CEO phase-lock could not be achieved in this GHz-frequency comb via pump modulation.

With our feedback loop (Fig. 4) it was possible to apply an appropriate feedback to the current of the multi-spatial-mode laser diode to achieve a tight phase-lock of f_{CEO}. The microwave spectrum of the phase-locked CEO beat is depicted in Figs. 5(c) and (d). When

phase-locked, a coherent peak appears in the microwave spectrum with a linewidth only limited by the resolution bandwidth of the spectrum analyzer. The drastically reduced CEO frequency noise PSD lies integrally below the β-separation line [36], confirming the phase-lock of the CEO beat (Fig. 5(a)). The in-loop residual integrated CEO phase noise shown in Fig. 5(b) amounts to 744 mrad [1 Hz, 5 MHz] despite the strongly multimode pumping scheme. At offset frequencies higher than 3 MHz, the noise is limited by the measurement shot-noise.
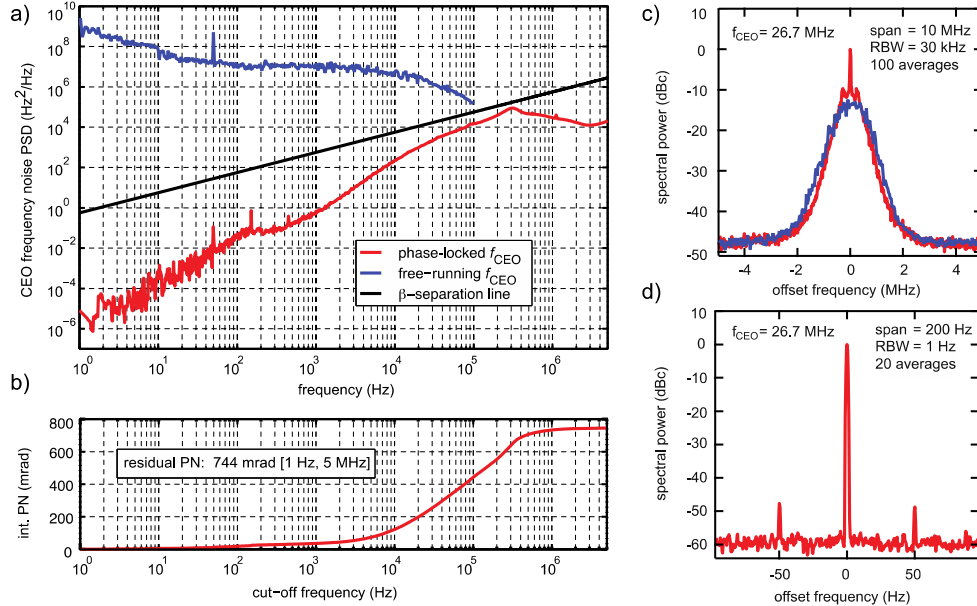

Fig. 5. Phase-locked f_{CEO}: (a) Measured frequency noise PSD of the free-running (blue) and phase-locked (red) CEO beat. The frequency noise power spectral density of the phase-locked CEO lies integrally below the β-separation line, confirming the tight phase-lock. (b) A low residual integrated phase-noise (PN) of 744 mrad in the integration bandwidth of [1 Hz, 5 MHz] is achieved; (c) Microwave spectrum of the phase-locked CEO beat with the central coherent peak (red) and the free-running CEO beat (blue) in a 10-MHz span (RBW = 30 kHz, 100 averages); (d) Zoom into the coherent CEO-peak in a 200-Hz span (RBW = 1 Hz, 20 averages).

Locking the CEO frequency also impacts the amplitude noise and timing phase noise of the GHz-laser (Figs. 6(a) and 6(c)). The intensity noise of the GHz-laser (Fig. 6(a), blue) mainly consists of $1/f$-noise at low frequencies (below 100 Hz) and of a significant white noise level above 100 Hz that we attribute to the multi-spatial-mode characteristics of the pump diode. This white noise at frequencies higher than ≈20 kHz is filtered by the low-pass behavior of the laser cavity originating from its photon lifetime and the effective upper-state lifetime of the gain. A similar noise spectrum was observed for the free-running CEO beat (see Fig. 5(a)). When the CEO frequency is locked, the white noise component in the laser intensity is drastically reduced by the feedback to the pump laser diode, which indicates that the same noise source is responsible for the noise in the CEO beat and laser intensity. However, the low-frequency $1/f$ component of the laser amplitude noise is unchanged when the CEO is phase-locked, indicating that this noise contribution is uncorrelated between the CEO and the laser intensity. An additional noise bump appears in the laser intensity noise when the CEO is stabilized, which corresponds to the servo bump of the PLL (Fig. 6(a), red). This servo bump indicates that a PLL bandwidth of ≈300 kHz is achieved, much larger than the bandwidth of the CEO frequency modulation via the pump current without a phase-lead

component. The laser intensity noise relative to the repetition rate carrier at 1 GHz, was reduced from 0.05% rms [1 Hz, 1 MHz] when the CEO beat was free-running to below 0.03% rms when the CEO frequency was phase-locked (Fig. 6(b)).
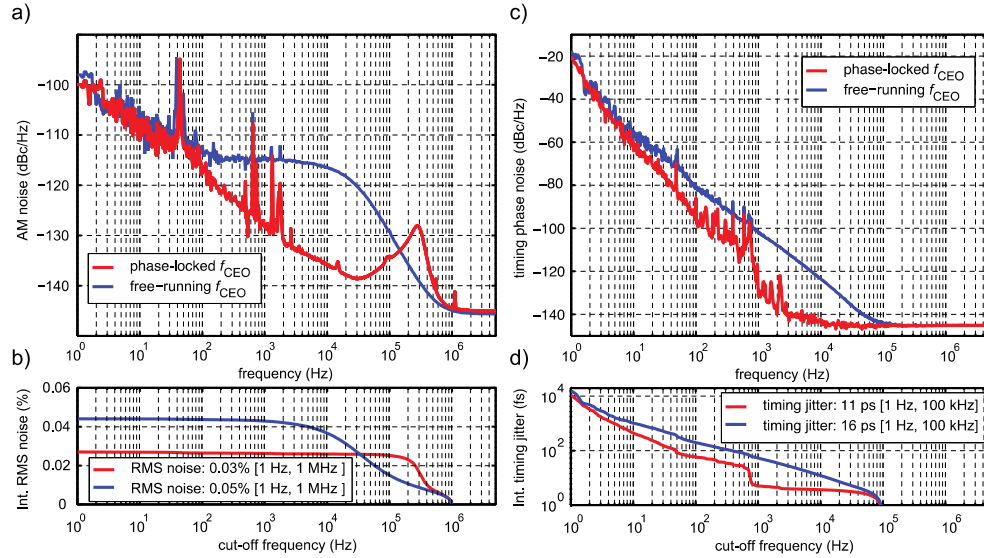

Fig. 6. CEO phase-locking impact on the noise of the 1-GHz CALGO laser: (a) Amplitude noise (no feedback: blue, while CEO-locked: red). (b) The rms amplitude noise [1 Hz, 1 MHz] decreases from 0.05% for the free-running laser to below 0.03% when f_{CEO} is phase-locked. (c) The timing phase noise of the pulse repetition rate (no feedback: blue, while CEO-locked: red) from the 1-GHz cavity, which is not actively stabilized in our experiment, reduces when f_{CEO} is tightly locked. (d) When the f_{CEO} is phase-locked the timing jitter of the laser reduces from 16 ps to 11 ps [1 Hz, 100 kHz]. No active stabilization of the frequency comb spacing (i.e. pulse repetition frequency) was done at this point.

In this experiment, the GHz-cavity was not actively stabilized against mechanical perturbations leading to a timing jitter of 16 ps [1 Hz, 100 kHz] when the laser was completely free-running. When the CEO frequency was stabilized with the PLL, the timing jitter was reduced to 11 ps. In Fig. 6(d) the timing jitters are shown for a continuous lower integration limit and a fixed upper limit of 100 kHz. In Table 1 the timing jitters of three different integration ranges are compared. This observation implies that the pump current has a coupled influence on both the CEO frequency and repetition rate of our GHz-laser, in a similar way as previously studied in details in an Er:fiber comb [37]. Deeper insights into this effect are expected when the laser repetition rate is actively stabilized using a piezo-controlled GHz-cavity, which is well established and much easier to be implement than the f_{CEO} stabilization (but requires a piezo-controlled cavity mirror and another feedback loop).

Table 1. Timing Jitters of the Free-running (blue) and CEO-locked (red) GHz Frequency Comb for Different Integration Ranges*

Integration range	GHz-CALGO free-running	GHz-CALGO CEO-locked
1 Hz to 100 kHz	16 ps	11 ps
10 Hz to 100 kHz	1 ps	438 fs
100 Hz to 100 kHz	198 fs	64 fs

*The timing jitter was calculated from the phase noise measurements of the pulse repetition rate shown in Fig. 6(c). The GHz cavity was not actively stabilized with a piezo-controlled mirror.

5. Conclusion

We have presented the first CEO-stabilized 1-GHz diode-pumped solid-state laser (DPSSL). The SESAM-modelocked Yb:CALGO laser delivers high-power ultrashort pulses directly from the gigahertz oscillator. Without the need for any pulse amplification or compression a coherent octave-spanning supercontinuum is generated. We achieved a tight CEO stabilization even though a multi-spatial-mode diode laser is used. Thus the gigahertz frequency comb presented here is based on a very compact and robust laser setup. Coupling only 400 mW of average output power into a photonic crystal fiber generated a coherent octave-spanning spectrum. Strong CEO beat signals were obtained using a standard f-to-$2f$ interferometer. By using a combination of digital and analog electronics, a tight phase-lock of f_{CEO} to an external microwave reference was achieved with a low in-loop residual integrated phase-noise of 744 mrad [1 Hz, 5 MHz].

Acknowledgments